Expert Opinion

informa
healthcare

Stimuli-responsive liposome-nanoparticle assemblies

Matthew R Preiss & Geoffrey D Bothun[†]
University of Rhode Island, Department of Chemical Engineering, Rhode Island Consortium for Nanoscience and Nanotechnology, Kingston, RI, USA

Introduction: Nanoscale assemblies are needed that achieve multiple therapeutic objectives, including cellular targeting, imaging, diagnostics and drug delivery. These must exhibit high stability, bioavailability and biocompatibility, while maintaining or enhancing the inherent activity of the therapeutic cargo. Liposome-nanoparticle assemblies (LNAs) combine the demonstrated potential of liposome-based therapies, with functional nanoparticles. Specifically, LNAs can be used to concentrate and shield the nanoparticles and, in turn, stimuli-responsive nanoparticles that respond to external fields can be used to control liposomal release. The ability to design LNAs via nanoparticle encapsulation, decoration or bilayer-embedment offers a range of configurations with different structures and functions.
Areas covered: This paper reviews the current state of research and understanding of the design, characterization and performance of LNAs. A brief overview is provided on liposomes and nanoparticles for therapeutic applications, followed by a discussion of the opportunities and challenges associated with combining the two in a single assembly to achieve controlled release via light or radiofrequency stimuli.
Expert opinion: LNAs offer a unique opportunity to combine the therapeutic properties of liposomes and nanoparticles. Liposomes act to concentrate small nanoparticles and shield nanoparticles from the immune system, while the nanoparticle can be used to initiate and control drug release when exposed to external stimuli. These properties provide a platform to achieve nanoparticle-controlled liposomal release. LNA design and application are still in infancy. Research concentrating on the relationships among LNA structure, function and performance is essential for the future clinical use of LNAs.

Keywords: controlled release, electromagnetic, liposome, nanoparticle, photothermal

Expert Opin. Drug Deliv. (2011) 8(8):1025-1040

1. Introduction

A significant challenge faced today in drug discovery is that many promising therapeutics have poor pharmacological properties, making them unsuitable for use in their native forms [1]. Some estimate that > 95% of new drug candidates fail to have the pharmacokinetic properties needed to be an effective treatment [2]. Improving pharmacokinetics requires chemically modifying the drug, for instance, to make it water soluble, or physically modifying it by mixing or encapsulating it within a suitable matrix. Disconnect between drug discovery and drug delivery is one of the biggest reasons for the decline in breakthrough drugs in recent years [1]. New nanotechnology-based drug delivery systems have shown great potential for overcoming obstacles related to poor pharmacokinetics by providing a mechanism for controlling the delivering of low drug dosages to specific tissues or cells [3,4]. Targeted and controlled delivery can reduce the adverse effects of systemic delivery

10.1517/17425247.2011.584868 © 2011 Informa UK, Ltd. ISSN 1742-5247

Article highlights.

- Review of recently reported liposome-nanoparticle assemblies (LNAs) designed for stimuli-responsive controlled-release. Radio frequency-triggered magnetoliposomes are a classic example of a stimuli-responsive LNA. In recent years, there has been an increased interest in LNA designs utilizing light-responsive nanoparticles, such as gold nanoparticles.
- Three distinct strategies are used to design LNAs: nanoparticle encapsulation, bilayer-embedment or surface decoration. With each design, nanoparticle–liposome interactions must be considered as they play a role in LNA structure and stability.
- Intuitively, LNA release in the presence of an electromagnetic field is enhanced when the nanoparticle is closely associated with the bilayer. Examples are presented from the literature for iron oxide and gold nanoparticles.
- LNA release is commonly attributed to local nanoparticle heating; however, mechanically-induced release may be more plausible.

This box summarizes key points contained in the article.

and off-target affects. The dream of Nobel Laureate Paul Ehrlich's 'magic bullet' may be within reach through controlled and targeted nanoscale therapeutics.

In 2005, the National Cancer Institute provided a vision for nanotechnology-based cancer treatment that combines targeted delivery with imaging, diagnostics and the ability to provide multiple therapies within a single nanoscale construct [5]. The design of such a multifunctional construct is inherently complex as it requires combining different molecular, colloidal and/or particulate agents that, for example, may have different degrees of hydrophobicity or thermal instability. Furthermore, the construct must be colloidally stable, resist protein adsorption and immune system recognition, and achieve cellular targeting in its native form (i.e., without 'losing' components or cargo during circulation).

Liposome-nanoparticle assemblies (LNAs) represent a promising route for designing multifunctional therapeutic constructs. They draw inspiration from magnetoliposomes (MLs) (liposomes containing encapsulated magnetic nanoparticles (NPs) [6-11]) and have also been referred to in recent literature as liposome–NP hybrids or liposome–NP complexes [12,13]. LNAs consist of liposomes that contain NPs encapsulated in the aqueous core, embedded in the lipid bilayer or bound (decorated) onto the surface (**Figure 1**). While liposomes and NPs have both been approved separately for clinical use, research and development of LNAs are still relatively new. Liposomes are attractive for drug delivery and biomedical imaging because they are biocompatible carriers capable of protecting and transporting hydrophobic and/or hydrophilic therapeutic molecules. NPs (up to 100 nm) have also been shown to be effective transporters, contrast agents and agents capable of providing *in vivo* heating when subjected to external stimuli such as alternating current electromagnetic fields (EMFs; typically at radiofrequencies, RF) or light [14-19]. LNAs can incorporate the intrinsic properties of liposomes and NPs, providing novel multifunctional therapeutic and diagnostic vehicles. This concept was depicted by Pradhan *et al.* [20] for folate (Fol) receptor and magnetically targeted MLs capable of combined drug delivery and hyperthermia (**Figure 2**). Principle advantages of LNAs include the following:

- Delivery of hydrophobic and hydrophilic molecules and NPs, including small NPs (< 25 nm) that are less prone to endocytic uptake due to the high curvature energy required for a membrane to 'wrap' around the particle [21].
- Strategies for processing, stabilizing and targeting liposomes are well established [22].
- NPs can be magnetically guided for targeting *in vivo* and provide a triggering mechanism for controlled release (not discussed in detail herein).
- Surface-bound NPs can also enhance the colloidal stability of LNAs and bilayer-embedded NPs can reduce spontaneous leakage [23-26].

The objective of this article is to provide a detailed review of LNA design and structure with an emphasis on recent work that utilize photothermal (via gold NPs) or RF heating (via iron oxide NPs) to achieve hyperthermia treatment, controlled drug release, or combined hyperthermia and drug release. LNAs containing carbon fullerenes such as C_{60} of C_{70} (i.e., fullerenosomes, [27-36]) are promising therapeutic structures and provide insight into LNA design, but are not discussed herein. Likewise, NPs containing supported lipid bilayer (SLB) coatings are also quite promising, but are not discussed (e.g., [7,37-39]). A discussion of reported LNA performance *in vitro* and *in vivo* is provided. This compliments a review of 'liposome-nanoparticle hybrids' by Al Jamal and Kostarelos in 2007 [12]. Recent reviews focusing on liposomes or NPs for therapeutic application, which are discussed only briefly herein, are provided in [22,40-43] and [4,15-17,44-48], respectively. An expert opinion is provided that focuses on the need for more complete design principles, additional characterization of LNA structure and stability, and the validity of local heating.

1.1 Liposomes

Since the pioneering work by Bangham *et al.* and Papahadjopoulos and Ohki in the 1960s [49-51], liposomes have become a well-established platform for administering therapeutic and imaging agents. In 1973, Gregoriadis reported the potential of liposome-aided drug delivery and started what would become a burgeoning new field of liposomes as nanoscale delivery vehicles [52]. Since then, liposomes have become one of the most reliable systemic drug delivery systems,

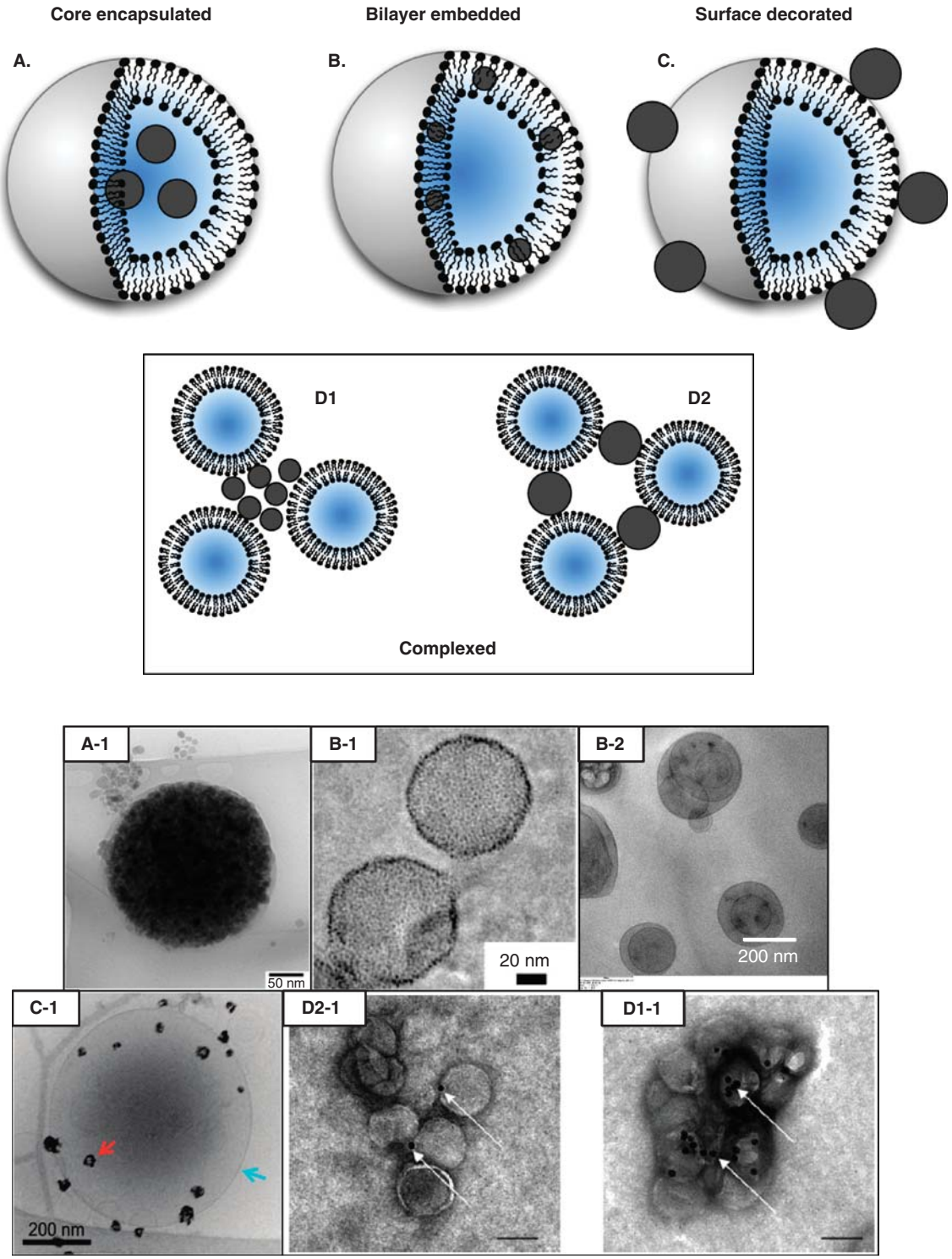

Figure 1. Schematic and TEM micrographs of LNAs formed by encapsulated hydrophilic nanoparticles with an aqueous liposome core (A; A-1 [70]**),** embedding hydrophobic nanoparticles within a liposome bilayer **(B; B-1** [82]**, B-2** [23]**)** or binding hydrophilic nanoparticles to a liposome surface **(C; C-1** [92]**)**. Surface decoration **(C)** can also be used to create controlled aggregates or complexes **(D; D1-1, D2-1** [13]**)**. Structures and proportions are not to scale.

Reprinted from [13,23,70,82,92] with permission.

LNA: Liposome-nanoparticle assembly.

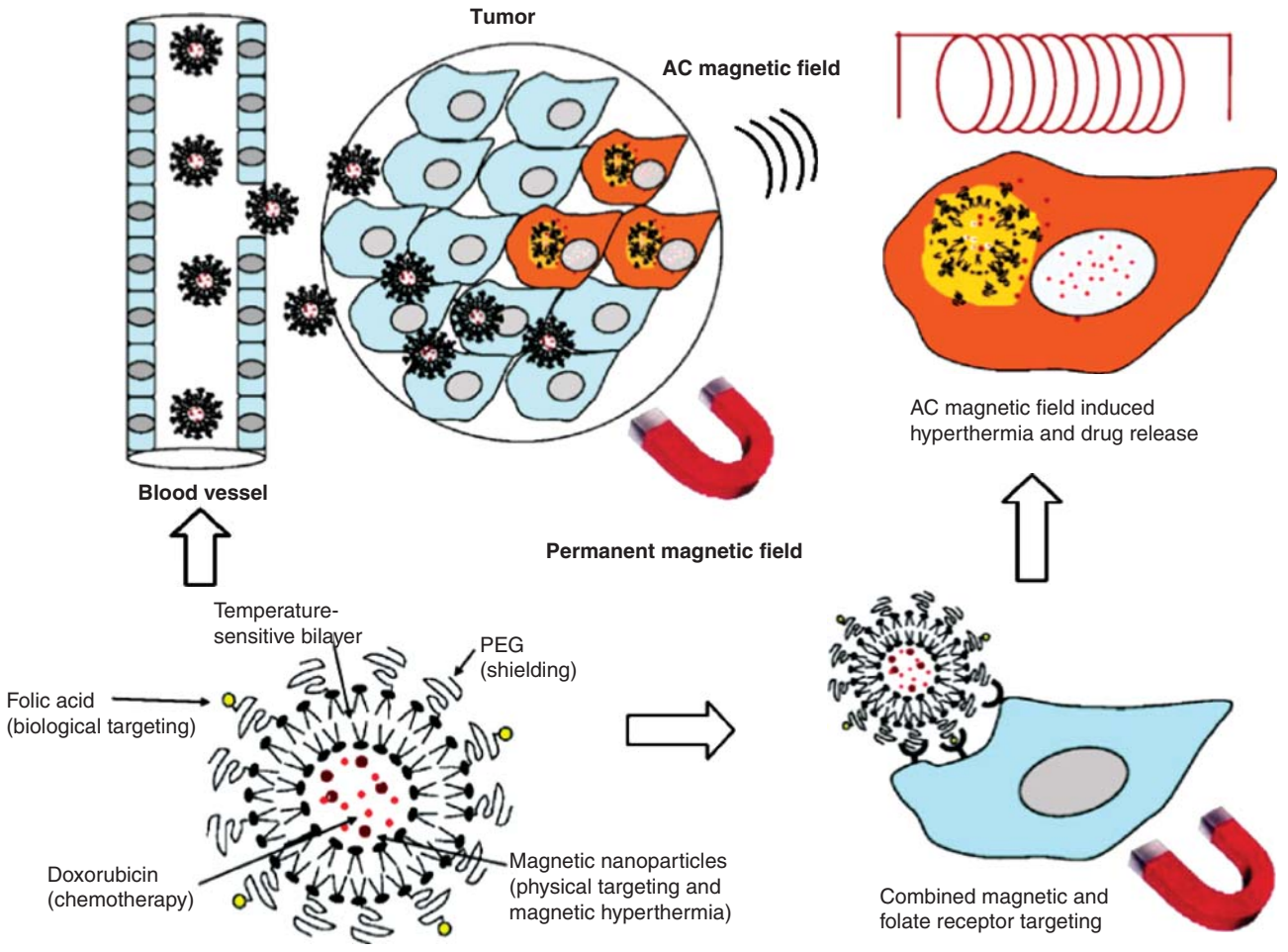

Figure 2. The concept of a multifunctional LNA (a temperature sensitive magnetoliposome containing co-encapsulated iron oxide nanoparticles and doxorubicin) for cancer thermo-chemotherapy from Pradhan *et al.* [20]. Passive targeting can be achieved through the EPR effect of tumor vasculature, and active targeting can be achieved via folate receptor and by applying a permanent magnetic field. The application of an AC electromagnetic field can be used to release the drug and achieve hyperthermia treatment.

Reprinted from [20] with permission.

AC: Alternating current; EPR: Enhanced permeation and retention; LNA: Liposome-nanoparticle assembly.

particularly because of their biocompatibility and ability to reduce or prevent drug degradation and toxicity.

Liposomes are self-assembled spherical vesicles consisting of one (unilamellar) or multiple (multilamellar) lipid bilayers surrounding an internal aqueous core. Bilayer thickness (l_b) is ~ 5 nm, of which ~ 3 nm is the acyl lipid tail region. Liposomes can be prepared with zwitterionic, anionic or cationic lipids, and the net liposome surface charge can be adjusted by mixing different ratios of these components. Lipids with headgroup-conjugated PEG and ligands can be used to improve liposome stability, increase blood circulation times and achieve cellular targeting [22,41]. For drug delivery and diagnostics, liposomes are attractive because of their ability to encapsulate both hydrophilic (in the aqueous core or bound to the liposome surface) and hydrophobic (in the lipid bilayer) molecules. This enhances the solubility and stability of these molecules and prolongs their bioavailability.

Release of encapsulated molecules from liposomes is controlled by the permeability through the lipid bilayer, which can be achieved by transbilayer diffusion or transient pore formation triggered by bilayer disruption or phase separation. Phase separation can be induced by 'melting' the liposomal bilayers, that is, heating to a temperature greater than the characteristic main phase transition or melting temperature of the lipids (T_m). Below T_m, the lipids are in the solid or gel phase in which the lipids are rigid and highly organized. Above T_m, the lipids are disordered in a liquid crystalline or fluid phase. Permeability is high at the interface between gel and fluid phases. Phase separation and bilayer permeability can be manipulated by adjusting the lipid bilayer

composition. A simple example illustrating this principle can be made with dipalmitoylphosphatidylcholine (DPPC, T_m = 42°C) and dimyristoylphosphatidylcholine (DMPC, T_m = 23°C). At a DPPC:DMPC molar ratio of 74:26, the melting temperature occurs at physiological temperature (37°C). Furthermore, cholesterol is commonly incorporated into the bilayer to reduce membrane fluidity above the melting temperature. Membrane fluidity is affected by, for example, pH, ion concentration and the presence of molecules absorbed into the bilayer.

Drug delivery from liposomes is accomplished by cellular uptake, which can occur by adsorption, endocytosis, fusion and/or lipid transfer [41,42,53]. Adsorption is the association of liposome bilayer with cell bilayer without destroying the liposome bilayer or being internalized by the cell. Adsorption can be specific (assisted by targeting ligands such as antibodies) or nonspecific (controlled by intermolecular and surface forces). Endocytosis involves the uptake of liposomes into the cell by encapsulation within endosomes. Release of drugs to the cytoplasm can occur by membrane destabilization of the encapsulating endosome or by delivery to lysosomes. Lysosomes have an acidic pH and contain lysing enzymes. Drug release is accomplished when lysosome enzymes hydrolyze the lipid bilayer releasing the drug. Lysosome drug release is only effective when the encapsulated drugs are not susceptible to lysosome enzymes and pH. Fusion involves the adsorption and incorporation of the liposome bilayer with the cell membrane, releasing the payload into the cytoplasm. Finally, lipid transfer involves the exchange of lipids between the liposome bilayer and the cell membrane without enveloping the liposome [41,42].

1.2 Gold and iron oxide nanoparticles

Imaging and photothermal effects of gold NPs stem from their enhanced surface plasmon resonance (SPR), where visible or near-infrared light is absorbed causing oscillation of surface electrons [54]. SPR absorbance and the wavelength range are dependent on NP size, core/shell configuration (e.g., silica core/gold shell [55]) and geometry. Shifts in these properties are indicative of the degree of NP aggregation and/or molecular adsorption on the NP surface [19]. For photothermal therapy, absorbed light energy is converted into local heat that thermally diffuses into the surrounding medium. Varying NP size and core/shell configuration provides a means of tuning the frequency window for photothermal therapy. It is generally accepted that gold NP-mediated phototherapy is attributed to heat or resulting bubble nucleation depending on the light intensity and mode of exposure [19]. However, recent work by Krpetic *et al.* [56] at low light energies suggests that photochemical effects – the formation of free radicals during NP irradiation – may play an important role. In addition to photothermal heating, EMFs operating at RF can also be used to heat gold NPs. For example, Gannon *et al.* [57] examined the effect of NP concentration and RF field strength on the heating rates of 5 nm Au NPs in water. A rate of ~ 74°C min^{-1} was measured using an 800 W RF field at an NP concentration of 67 μM.

The magnetic properties of iron oxide NPs, notably single domain superparamagnetic magnetite (γ-Fe_2O_3) or maghemite (Fe_3O_4), can also be exploited for imaging and therapy. They act as contrast agents for MRI, can be directed by static magnetic fields (magnetic drug delivery) and can be heated by RF (hyperthermia) [16,18,58]. RF heating is due to magnetic losses being converted to heat, typically at low frequencies between 100 and 400 kHz. The magnetic losses for NPs < ~ 30 nm are due to Néel relaxation, arising from rapidly alternating magnetic dipole moments, and Brownian relaxation, arising from NP rotation and viscous losses (friction). RF heating is advantageous because it is non-invasive, easily penetrates the body and is physiologically acceptable for up to 1 h if the product *Hf*, where *H* is the field amplitude (current × number of coils per length) and *f* is the frequency, is below 4.85 × 10^5 kA m^{-1} s^{-1} [59]. NP heating capability is based on the inherent specific absorbance rate (*SAR*, W g^{-1}) of the NPs:

$$SAR = \frac{c_P}{m_{NP}} \frac{\Delta T}{\Delta t} \quad (1)$$

where c_p is the average heat capacity of the sample, m_{NP} is the NP mass and $\Delta T / \Delta t$ is the initial heating rate of the sample. *SAR* values up to ~ 700 W g^{-1} can be obtained depending on the NP size, composition and surface coating [18].

1.3 Nanoparticle-mediated hyperthermia

NPs capable of RF or photothermal heating have been used for local hyperthermia treatment of malignant tissues, which involves heating the tissues to temperatures between ~ 40 and 45°C [60]. During hyperthermia, heat denatures intracellular proteins inducing death by necrosis or apoptosis. Hyperthermia has also been shown to make tumor cells more vulnerable to therapies, such as chemotherapy and radiotherapy; therefore, it can be used in conjunction with these therapies [20,61-62]. The use of conventional hyperthermia (i.e., without NPs) has been tempered in recent years because of difficulty in applying heat to deeper tumors and delivering targeted heating. This difficulty may be addressed by targeting NPs to malignant cells and tissues.

Heat transfer within tissues via NP heating can be described by a modified Pennes' bio-heat transfer model [63]:

$$\rho_t c_{p,t} \frac{\partial T}{\partial t} = \nabla \bullet (k_t \nabla T) + \rho_b c_{p,b} \omega_b (T - T_b) + Q_m + Q_{NP} \quad (2)$$

where ρ_t is the tissue density and $c_{p,t}$ is the tissue heat capacity. The first term on the right hand side (RHS) of the equation describes the conductive heat transfer (k_t is the tissue thermal conductivity) and the second term describes the convective heat transfer (ρ_b is the blood density, $c_{p,b}$ is

the blood heat capacity, ω_b is the blood perfusion rate and T_b is the blood temperature). Q_m is the rate of heat generated metabolically and Q_{NP} is the rate of heat generated from the power dissipation by the NPs, which accounts for the concentration of NPs (e.g., Q_{NP} represented as *SAR*). Equation 2 represents the case where the temperature profile in a tissue mass (macro-scale) can be determined as a function of NP concentration and applied field strength (e.g., laser or RF). It has been shown theoretically that sufficient iron oxide NP heating can be achieved (> 42°C) at low blood perfusion rates to achieve tissue-level hyperthermia [64]. For cellular-level heating (nano- or micro-scale), convective heat transfer due to blood transfusion and Q_m are eliminated from Equation 2, yielding the expression reported by Keblinski *et al.* [65] for RF NP heating and Xu *et al.* [66] for Fe_3O_4 NP hyperthermia *in vitro*.

2. LNA formation and structure

LNA design strategies include the encapsulation of individual or multiple NPs within the aqueous core of the liposome, embedding hydrophobic NPs in the lipid bilayer, and binding or conjugating NPs to the liposome surface (**Figure 1**). **Tables 1** and **2** contain a list of Au and iron oxide LNAs, respectively, that have been reported in the literature since 2008. For a given design strategy, the functionality of an LNA is determined by the liposome composition, the type of NPs used, the intermolecular and surface interactions between the lipid bilayer and NP, and (as in all cases) the colloidal stability. LNAs can be used to concentrate NPs and shield them from the adsorption of exogenous molecules. Concentrating the NPs can increase the degree of intracellular delivery, which is critical, for example, in imaging and hyperthermia applications. In turn, shielding the NPs from the adsorption of biomolecules can enhance their bioavailability and reduce the need for more complex NP surface chemistries. The caveat here, which is germane to all LNA configurations, is that the liposome itself must contain functional lipids or surface coatings for stabilization and, when needed, targeting [12].

In addition to serving as a vehicle for NP delivery and being multifunctional, LNAs can be used to overcome design challenges of 'conventional' liposomes. With respect to delivery, the main challenge includes creating an assembly that is stable and retains its cargo during both storage and circulation, but is capable of releasing its cargo *in vivo* at a target site (i.e., stable until it needs to become unstable). This challenge has been addressed by using lipid mixtures that melt near physiological temperature or through chemical mechanisms such as pH-sensitive lipids; which has ultimately reduced the number of viable lipid molecules that can be used. In contrast, LNAs can utilize physical triggers, predominantly NP heating, to control the onset and duration over which a molecule is released. While lipid composition plays an active role in determining the release profile from LNAs, the lipids themselves would not provide the release trigger. This could greatly expand the range of lipids amenable to liposomal release [12].

Finally, LNAs can potentially be used to deliver high concentrations of NPs capable of RF or photothermal heating for local hyperthermia. Targeted LNA administration can be achieved through known liposomal-based mechanisms (e.g., targeting lipids) and may provide a local heat source for both hyperthermia and drug release without adversely effecting adjacent tissue.

2.1 Core encapsulation

Encapsulating inorganic NPs within the aqueous core of liposomes is one of the simplest and earliest developed LNA configurations (e.g., MLs [7,9]). They can be prepared by encapsulating preformed NPs in solution or by forming NPs within the liposome core as first shown by Papahadjopoulos and co-workers in 1983 [67]. The later approach will not be discussed herein. Encapsualted LNAs (e-LNAs) can be prepared by thin film hydration (TFH), double emulsion (DE) [68] or reverse phase evaporation (REV) [69]. Prior to removing unencapsulated NPs or diluting, post-formation liposome processing such as membrane extrusion or sonication can be used. The obvious design constraints are that the NPs must be colloidal stable during LNA formation and that their diameter (d) must be less than that of the aqueous liposome core. When $d_{core} = d_{NP}$, these structures are referred to as SLB (i.e., NPs containing a lipid bilayer coating). Based on close packing of spheres and $d_{core} >> d_{NP}$, the maximum theoretical number of encapsulated NPs is $n \approx 0.74$ (V_{core}/V_{NP}) where V represents the volume of the core or NP. Wijaya and Hamad-Schifferli [70] have shown that it is possible to approach this limit, demonstrating high-density encapsulation of Fe_3O_4 NPs (d_{NP} = 12.5 nm) within DPPC liposomes (**Figure 1A-1**). With this design, the available core volume for co-encapsulating aqueous drug molecules decreases within increasing NP concentration. However, the ability for embedding hydrophobic molecules within the bilayer is unaffected by NP concentration.

The structure of e-LNAs is dependent on the osmotic pressure differential across the lipid bilayer, and the attractive or repulsive forces between the bilayer and the NPs. The elasticity of the bilayer determines how the LNA will deform in response to these forces. Attractive forces can include van der Waals, hydrophobic and electrostatic interactions; and repulsive forces can include electrostatic, depletion, hydration and steric interactions. As classically described by Lipowsky and Döbereiner [71], adhering and non-adhering NPs can lead to changes in bilayer curvature, which can impact liposome size, shape and phase homogeneity. This occurs when different particles are present within (i.e., encapsulated NPs) and outside (e.g., sugars or proteins) liposomes. For non-adhering encapsulated particles, the bilayer can curve towards the larger particles. In contrast, for small adhering encapsulated particles (attractive) where $d_{core} >> d_{NP}$ and $d_{NP} < 2l_b$, the bilayer can curve away from the particles. For large

Table 1. Reported LNAs based on Au NPs since 2008.

Lipids (ratio)*	Liposome charge	NP diameter (nm)	Surface coating	Lipid:NP*	Association	Ref.
DOPC:DOTAP (8:2)	Cationic	80	Citrate	n.r.‡	Encapsulation	[91]
DPPC:DSPC (9:1)	Zwitterionic	2.5	Hexanethiol	17.2:1 (w/w)	Embedment	[95]
EggPC	Zwitterionic	2	Dodecanethiol	100:1 – 1500:1	Embedment	[82]
DPPC:DSPC (9:1)	Zwitterionic	4	Mercaptosuccinic acid	10:1 (w/w)	Encapsulation	[95]
DPPC:DSPC (9:1)	Zwitterionic	1.4	DPPE-Nanogold™	n.r.	Embedment/ decoration	[24]
DOPC DOPC:DOPC+ (90:10) DOPC:DOPP (9:1)	Zwitterionic Cationic Anionic	n.r.	Ascorbic acid	n.r	Decoration	[87]
EYPC EYPC:DDAB (9:1) EYPC:PEG-DSPE (95:5)	Zwitterionic Cationic Zwitterionic	13	Citrate	10:1, 1:1	Decoration	[88]
EggPC:DOTAP (9:1 w/w)	Cationic	4	Mercaptopropionic acid	$\geq 3.6 \times 10^{-3}$:1	Decoration	[89]
DPPC:DPTAP:Chol (6:3:1 w/w)	Cationic	20	n.r.		Complexation	[13]
DPPC	Zwitterionic	33	PEG	1.8:1 (w/mol) 1:1 (w/mol)	Encapsulation Embedment/ decoration	[92]

*Molar ratios provided unless noted otherwise.
‡Estimated at 4 liposomes per NP.
LNA: Liposome-nanoparticle assembly; NP: Nanoparticle; n.r.: not reported.

Table 2. Reported LNAs based on iron oxide NPs since 2008.

Lipids (ratio)*	Liposome charge	NP diameter (nm)	Surface coating	Lipid:NP*	Association	Ref.
Magnetite (Fe_3O_4)						
DPPC:Chol (75:25)	Zwitterionic	12.5	ND	0.8:1	Encapsulation	[98]
[maleimide]PEG-DSPE:FAM-DOPE (10:1 w/w)		10 – 14	Heptanioc acid, acetic acid	1:1.8 (w/w)	Encapsulation	[99]
DMPC:Chol:XL‡ (47.5:47.5:5) DPPC:DMPC:XL‡ (9.5:85.5:5)	Zwitterionic	10	Catechol	≥ 8.3:1 (mol/w)	Complexation	[90]
Maghemite (γ-Fe_2O_3)						
DPPC:Chol (67:33)	Zwitterionic	10	Glutamic acid	n.r.	Encapsulation	[100]
DPPC:Chol (5:1, 15:3 w/w) DPPC:DSPC:Chol (10:5:3 w/w)	Zwitterionic	43	Dextran	n.r.	Encapsulation	[93]
DPPC	Zwitterionic	5	Oleic acid	1000:1 – 10,000:1	Embedment	[23]

*Molar ratios provided unless noted otherwise.
‡Crosslinking molecule (adhesive lipid).
LNA: Liposome-nanoparticle assembly; NP: Nanoparticle.

adhering particles where $d_{NP} >> 2l_b$, the bilayer can curve around or engulf the particles. Given that NP adhesion to bilayers can significantly alter LNA structure and morphology, LNAs with encapsulated NPs are generally formed with small non-adhering NPs. The exception to this is LNAs formed by coating a single large NP with an adsorbed or SLB (not discussed herein).

Pradhan *et al.* [72] compared the encapsulation efficiency of 10 nm Fe_3O_4 NPs coated with lauric acid in LNAs (or more specifically MLs) composed of egg PC:cholesterol (1:0 to 1:2, molar ratio) and formed by TFH and DE. This represents a non-adhesive system. In general, higher encapsulation efficiency was achieved by TFH compared to DE. This was attributed to NP aggregation due to lauric acid stripping from the NP surfaces during the DE process. In both cases, the observation that an egg PC:cholesterol ratio of 2:1 yielded the best encapsulation efficiency (70% via TFH) was attributed to cholesterol inducing a single liquid ordered bilayer phase. Changes in liposome size on encapsulation were not reported.

In similar work, Sabate *et al.* [73] examined the effect of Fe_3O_4 NP concentration coated with tetramethylammonium hydroxide (58 nm hydrodynamic d_{NP}) on the encapsulation efficiency of extruded soybean PC MLs. This represents an adhesive system. The encapsulation efficiency decreased from 96.6% at 1.22 g Fe_3O_4/mol PC to 18.5% at 119.95 g Fe_3O_4/mol PC. This was attributed to electrostatic interactions (attraction) between the cationic NPs and the PC bilayers. The size of the MLs increased from 140 to 197 nm, consistent with lower curvature due to NP adhesion at the inner bilayer surface.

Gomes *et al.* [74] prepared polyelectrolyte-coated MLs by encapsulating 8 nm anionic γ-Fe_2O_3 NPs within egg PC liposomes and then coating with alternating poly(allylamine hydrochloride) and poly(sodium 4-styrenesulfonate) layers. The final coating determined the surface charge (anionic PSS or cationic PAH). The size ranged from 200 to 400 nm and the polyelectrolyte coating stabilized them against detergent-induced leakage, which is caused by membrane disruption or solubilization.

2.2 Bilayer embedment

Embedding NPs into the bilayer requires that the NPs be hydrophobic and have diameters comparable to or smaller than the thickness of the lipid bilayer (~ 5 nm; **Figure 1B**). LNAs formed by bilayer embedment (b-LNAs) can be advantageous as many NPs are inherently hydrophobic or synthesized in organic solvents (e.g., in reverse microemulsions where the surfactant is the initial surface coating) before undergoing surface modification for aqueous environments. Similar to the ability of cells to accommodate membrane proteins, liposomes can distort to accommodate hydrophobic NPs that exceed the thickness of hydrophobic acyl region of the bilayer (~ 3 nm) [23,75-77]. As with proteins, embedded NPs can affect lipid packing, lipid phase behavior, transbilayer permeability, and LNA structure and morphology [23,28,34,76,78-82]. A unique aspect of b-LNAs (as well as surface decorated LNAs (d-LNAs)) is that the NPs can provide direct localized heating to the bilayer in the presence of external stimuli to trigger release [23,24].

It is intuitive that the size of an NP (core + surface coating) and its concentration, or more specifically the lipid:NP ratio, will influence how the lipid bilayer distorts to accommodate it and the resulting LNA structure (**Figure 3**). Theoretical studies by Ginzburg and Balijepalli [83] and Wi *et al.* [84] suggest that the maximum size of an NP (d_{NP}) that can be incorporated into a LNA while maintaining a lipid bilayer structure is ~ 6.5 nm (**Figure 3A and B**). Above this size, micellar structures are more energetically favorable due to high local curvature strain within the bilayer [84]. Experimental verification of this critical size and, furthermore, the general size effects of NPs on embedment mechanism and LNA structure are more elusive.

Clustering of embedded NPs has been observed by Rasch *et al.* [82] in LNAs with dodecanethiol-coated Au (d_{NP} = 1.6 – 1.8 nm) (**Figure 1B-1**; **Figure 3A**). They showed that high NP loading with uniform distribution can be achieved in PC liposomes via TFH (with sonication and extrusion). Janus particles can be prepared with embedded NPs clustered in approximately a half of the liposomes via detergent loading followed by dialysis. Clustering occurs as the liposomes minimize the energy penalty for bilayer deformation, that is, for a given concentration of embedded NPs the periodic bilayer bending energy needed to accommodate individual particles is greater than that needed to accommodate NP clusters. Park *et al.* [80] and Chen *et al.* [23] have observed a similar clustering phenomenon with stearylamine-coated 3 – 4 nm Au and oleic acid-coated 5 nm γ-Fe_2O_3 NPs in DPPC liposomes (**Figure 1B-2**), respectively. This suggests that NP clustering is not restricted to d_{NP} < 2 nm [23].

In addition to clustering, embedded NPs with d_{NP} = 2 – 6.5 nm can reside in bilayer 'pockets' within individual (**Figure 3B**) or neighboring (**Figure 3C**) LNAs. These cases arise when the lipid:NP ratio is high (~ 1000:1 or greater). This has been observed by Jamal *et al.* [85] for 4 nm hydrophobic CdSe/ZnS core/shell quantum dots in DOPC bilayers.

2.3 Surface decoration and complexation

d-LNAs are formed when hydrophilic NPs are absorbed onto or coupled to the outer or inner surface of the lipid bilayer (**Figure 1C**). This is achieved through attractive surface interactions, notably long-range electrostatic attraction. An advantage of d-LNAs is the ease in which they can be prepared, adding NPs to pre-existing liposome dispersions. Similar to bilayer embedment, decorated bilayers also provide direct heating to the bilayer in the presence of external stimuli. The design constraint for forming d-LNAs is dependent on bilayer NP adhesion and curvature. NPs with d_{NP} > ~ 20 nm lead to the formation of SLBs due to liposome adsorption and rupture, followed by the bilayer curving around the particle. The critical NP diameter under which d-LNAs can be formed is $d_{NP} < 2(2k_b/w)^{1/2}$, where k_b is the bilayer bending elasticity, which is dependent on lipid composition and phase state, and w is the adhesion energy.

The Granick group has shown that stable d-LNA dispersions can be formed using zwitterionic liposomes with decorated cationic or anionic NPs (< 20 nm) with an NP surface coverage above ~ 25% [25,26]. This was achieved by electrostatic attraction. Lower surface coverage led to aggregation, which demonstrates the need to balance the lipid:NP ratio. It was shown that on binding the NPs could restructure the lipid bilayer, inducing gel phases in fluid liposomes and fluid phases in gel liposomes [86]. This observation shows that, even without external stimuli, bound NPs can induce changes in lipid phase behavior and, presumably, permeability.

Sau *et al.* [87] have also used electrostatic binding to prepare d-LNAs with Au NPs. High NP surface coverage was

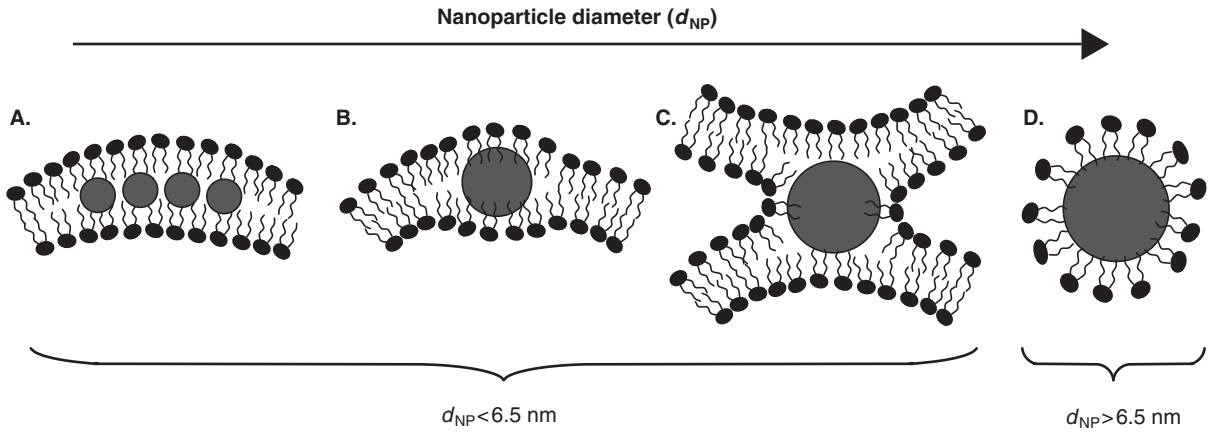

Figure 3. Changes in bilayer embedment mechanism with increasing nanoparticle diameter (d_{NP}, particle core + surface coating). (A) Small nanoparticles (defined herein as d_{NP} < 2 nm) cluster together to minimize bilayer bending energy [82]. **(B)** Larger nanoparticles (defined herein as d_{NP} = 2 – 6.5 nm) create 'pockets' within the bilayer or **(C)** bridge adjoining liposomes [23,77]. Above $d_{NP} \approx$ 6.5 nm, micellization is more energetically favorable than bilayer embedment [84].

achieved by using anionic Au NPs with physisorbed ascorbic acid and cationic liposomes (9:1 DOPC to ethyl-DOPC; T_m = -20°C). This high surface coverage was accompanied by NP aggregation due to the high local concentration and (probably) to charge screening via cationic lipids between bound particles (similar to Kojima *et al.* [88]). Binding was also achieved on zwitterionic and anionic liposomes with decreasing coverage (and NP aggregation), respectively. Pornpattananangkul *et al.* [89] have taken this one step further and have shown that pH can be used to control carboxyl-modified (anionic) Au NP binding to liposomes and, in turn, liposome stability. Above the pK_a of the carboxyl groups, the bound NPs stabilize the d-LNAs and prevent aggregation and fusion, while below the pK_a the NPs detach and liposome fusion resumes.

Last, LNAs can be formed by complexation (c-LNAs) if the liposomes surround NP aggregates (**Figure 1D1 and D2**) or the NPs bind to multiple liposomes and act as 'bridges' (**Figure 1D2**). Volodkin *et al.* [13] have shown that either structure can be formed from the same anionic Au NP-cationic liposome by manipulating electrostatic interactions via salt concentration. High NaCl concentration (75 mM) enhanced NP aggregation (**Figure 1D1-1**) and low salt concentrations inhibited it (**Figure 1D2-1**). In addition to non-specific physical interactions (electrostatic), crosslinking can be used to create c-LNAs. Mart *et al.* [90] used Fe_3O_4 NPs coated with histidine groups to bind to and complex zwitterionic–cholesterol liposomes containing Cu(iminodiacetate)-functionalized lipid. The objective was to demonstrate a potential method using histidine-Cu(IDA) binding to form c-LNAs, thereby concentrating a therapeutic and an imaging agent at a target site. The resulting aggregates ranged from 20 to 100 μm in diameter.

3. LNA-controlled release

This section reviews recent work on gold or iron oxide NP-mediated release from LNAs. Articles that apply these principles *in vitro* or *in vivo* are presented in Section 4.

3.1 Gold nanoparticles and photothermal effects

Utilizing the photothermal heating of Au NPs, Paasonen *et al.* [24] demonstrated the ability to control the release of calcein (622.6 MW) from Au LNAs composed of DPPC/DSPC at 9:1 (T_m = 44.9°C) with e-, d- and b-LNAs (**Figure 1A–C**). Leakage was examined with and without UV light at a wavelength of 250 nm over 30 min at 37°C. Without UV exposure, spontaneous calcein release was observed for e-LNAs with encapsulated mercaptosuccinic acid-coated NPs and b-LNAs with embedded hexanethiol-coated NPs. This was attributed to NP–lipid interactions at the bilayer–water interface and within the acyl tail region, respectively, which reduced bilayer integrity. With UV exposure, direct contact between NPs and the liposomes via bilayer-embedment led to the greatest release (~ 90% at 30 min). Intuitively, direct contact would improve the local heat transfer from the NPs to the liposomal bilayers relative to encapsulation. This led to a gel-fluid phase transition where calcein release was presumably enhanced by diffusion at the interface between coexisting gel and fluid domains.

Volodkin *et al.* [13] demonstrated the release of 5(6)-carboxyfluorescein (CF; 376.3 MW) from LNAs formed by the complexation of 128 nm cationic liposomes (DPPC/DPTAP/chol, T_m ~ 40 – 45°C) and 20 nm anionic Au NPs. Low NaCl concentration (7.5 mM) yielded LNAs with NP-mediated liposome bridges (**Figure 1D2-1**; type I) and high NaCl concentration (75 mM) yielded LNAs with

liposome-coated NP aggregates (**Figure 1D1-1**; type II). The type II LNAs were ~ 5 μm. CF release from type II LNAs was observed within 5 s after near-IR irradiation.

Anderson *et al.* [91] utilized the principle of plasmonic nanobubble (PNB) formation to control the release of 104 and 240 kDa proteins from cationic LNAs (~ 1 μm) containing encapsulated 80 nm anionic Au NPs. Irradiation was achieved using a single pump laser at 532 nm over 0.5 ns. Local vapor bubble formation led to mechanical disruption, as opposed to thermal, of the LNA bilayer and rapid protein release. The advantage of PNB formation is heating is isolated within the LNA triggering the immediate release of all encapsulated cargo.

Wu *et al.* [92] used hollow gold nanoshells (HGNs) encapsulated within or decorating the surface of DPPC liposomes to trigger CF release by near-IR pulses (800 nm) via microbubble formation and collapse (**Figure 1C-1**). LNA release was dependent on the proximity of the HGNs to the liposomes (decorated or tethered HGNs yielded the greatest response) and the laser power. Their results strongly suggest that release was attributed to transient disruption or poration of the lipid bilayer via transient bubble cavitation.

3.2 Iron oxide nanoparticles and alternating magnetic field effects

Tai *et al.* [93] examined CF release from thermosensitive zwitterionic liposomes containing encapsulated dextran-coated 43 nm γ-Fe_2O_3 NPs (Resovist™) using a high frequency generator (6.4 kW, 750 – 1150 kHz) operating for 5 – 25 min. CF release from DPPC:Chol (5:1) liposomes without encapsulated NPs was initiated between 35 and 37°C. In contrast, the LNA analogs exhibited initial release at 34 and 32°C with 7 and 14 mg Fe/ml, respectively. This initial release temperature was further tuned by increasing the cholesterol content (DPPC:Chol at 15:3) and incorporating a higher melting lipid (DSPC, T_m = 55°C). Release was attributed to NP heating. Using a rat model, they demonstrated that release could also be achieved *in vivo*.

Chen *et al.* [23] have recently examined the release of CF from LNAs formed with DPPC and bilayer-embedded oleic acid-coated 5 nm γ-Fe_2O_3 NPs at lipid:NP ratios of 10000:1, 5000:1 and 1000:1 as a function of RF energy (1 kW; 50 – 250 A, 281 kHz) (**Figure 4**). Experiments were conducted at non-invasive RF energies near or below 4.85×10^5 kA m^{-1} s^{-1} for 0 – 40 min [59]. The greatest release rate was observed at 5000:1, indicating an optimal NP loading for triggering release. This optimum reflected a balance between NP loading and LNA structure: high loading is needed for triggering bilayer release, but can lead to NP aggregation and can compromise LNA structure and stability. A unique observation was the fact that increasing NP loading reduced or eliminated spontaneous leakage by increasing bilayer stability. CF release was attributed to bilayer disruption via local heating and/or LNA rupture, which produced transient voids or pores.

4. LNA performance *in vitro* and *in vivo*

4.1 Cellular uptake and drug delivery

Chithrani *et al.* [94] prepared anionic Au decorated liposomes with 105 nm d_h by incorporating Au-conjugated DPPE (DPPE-Nanogold; 1.4 nm Au particles) into preformed DPPC/cholesterol liposomes. Incorporation of DPPE-Nanogold was confirmed by TEM and EDS. Liposome uptake by HeLa cells *in vitro* was independent of the DPPE-Nanogold concentration (2000:1, 1000:1, and 500:1 Au NPs per liposome). This key discovery suggests that the presence of DPPE-Nanogold does not influence cell uptake and that high NP loadings can be achieved in such LNAs without compromising internalization. Examining the intracellular fate revealed that the Au-liposomes were present in lysosomes and accumulated near the nuclear membrane after incubating for 45 min.

Paasonen *et al.* [95] examined uptake and light-induced calcein release of b-LNAs prepared hexanethiol-coated Au NPs (extension of [24]). The LNAs were composed of DSPC:DPPC (9:1 molar ratio) and were multilamellar with sizes ranging from 250 to 370 nm. *In vitro* studies with human retinal pigment epithelial cell line (ARPE-19) showed that the b-LNAs were internalized by endocytosis and localized in endosomes. Exposure to UV light at 400 mW/cm^2 for 300+ s led to calcein release from b-LNAs, but not from liposomes that did not contain embedded NPs.

4.2 Drug delivery and hyperthermia

Pradhan *et al.* [20] recently prepared folate (Fol) ligated MLs (e-LNAs) via TFH that contained co-encapsulated 60 nm iron oxide NPs and doxorubicin (DOX) in PBS. A proposed schematic of the e-LNA and the therapeutic concept is shown in **Figure 2**. The lipid components included DPPC, Chol, PEG_{2000}-DSPE and Fol-PEG_{2000}-DSPE, and the liposomes exhibited a melting temperature near 41°C. The liposomes were 361 nm in diameter and polydispersed (0.289), with an NP encapsulation efficiency of 24% (low, presumably attributed to the use of the TFH method). The liposomes exhibited temperature-dependent DOX release (more than twofold increase from 37 to 43°C). Fol-receptor targeted uptake was demonstrated in HeLa and KB cell cultures, and reductions in cell viability were attributed to a synergistic effect of DOX and hyperthermia treatment achieved in the presence of an AC EMF. While not mentioned specifically, we speculate that liposomal heating by the NPs may have aided DOX release.

Babincova and co-workers [96] prepared DPPC/PEG_{2000}-DSPE LNAs via REV that contained both dextran-coated Fe_3O_4 and C_{60} fullerene (referred to as magnetofullerenosomes) to achieve magnetic targeting and photodynamic therapy (PDT), respectively. Bis(di-isobutyloctadecylsiloxy)-2,3-naphthalocyanato silicon (isoBO-SiNc), a photosensitizing agent, was also encapsulated. LNA performance for treating B16 pigmented melanoma was examined *in vivo*

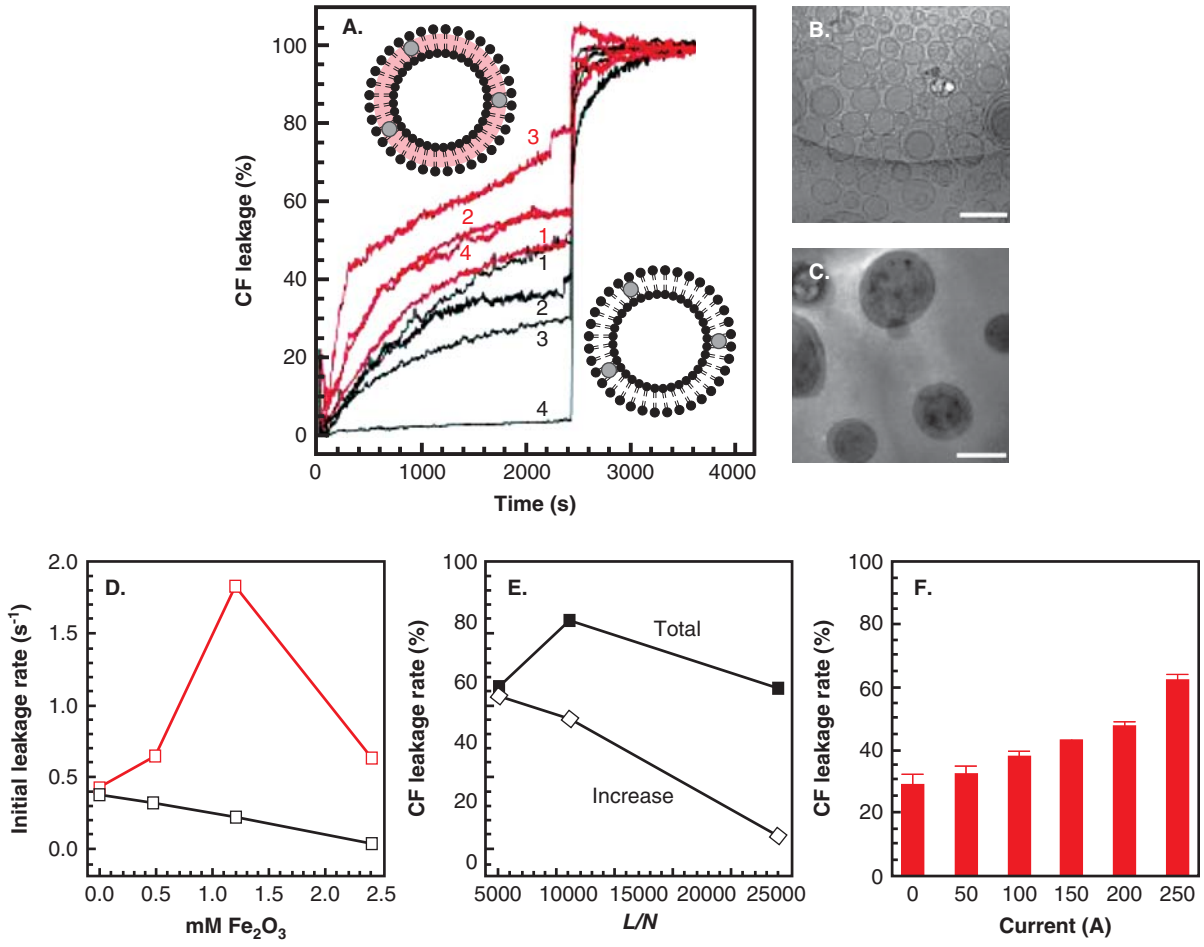

Figure 4. Controlled release of CF, a model encapsulated drug molecule, from magnetoliposomes consisting of 5 nm hydrophobic iron oxide NPs embedded within the bilayers of DPPC liposomes. (A) Release is shown with (red) and without (black) RF heating at 4.85 $\times$ 10^5 kA m^{-1} s^{-1} as a function of RF exposure. Images (**B**) and (**C**) show bare DPPC liposomes and the magnetoliposomes, respectively. The initial and total leakage is shown as (**D**) a function of iron oxide concentration and (**E**) the lipid:NP ratio (*L*:*N*), respectively. (**F**) Total CF leakage after 40 min of RF exposure could be varied with line current.
Reprinted from [23] with permission.
CF: Carboxyfluorescein; DPPC: Dipalmitoylphosphatidylcholine; NP: Nanoparticle; RF: Radiofrequency.

using a female mouse model. Without magnetic targeting, C_{60}-mediated PDT followed by isoBO-SiNc-mediated PDT led to a significant reduction in tumor growth over 19 days relative to no treatment or isoBO-SiNc-mediated PDT alone. When magnetic targeting was applied (0.32 T magnet placed on the tumor surface for 24 h), there was negligible tumor growth over the same duration.

5. Expert opinion

Liposomes or NPs for therapeutic application are well established and have been approved by the FDA for clinical use. The combination of these two systems in hybrid structures represents a unique opportunity for achieving multiple therapeutic objectives. The liposomes can act to concentrate small NPs and shield them from the immune system. In turn, the NPs can be used to initiate and control drug release when exposed to external stimuli. However, the design and use of LNAs is still in its infancy. This is apparent from the literature where, for example, NP loading is expressed in multiple ways (e.g., total concentration; lipid:NP molar or mass ratios; liposome:NP surface area ratio). Further studies in the design and use of LNAs are needed addressing the following questions:

- *How do physical and chemical interactions between NPs and the lipid bilayer affect LNA formation, structure and stability?* Encapsulated, decorated and embedded NPs can affect lipid ordering (ordering or disordering are possible) and alter bilayer phase behavior. Ordering or phase state affects the permeability and stability of LNAs. These effects will be dependent on the physical

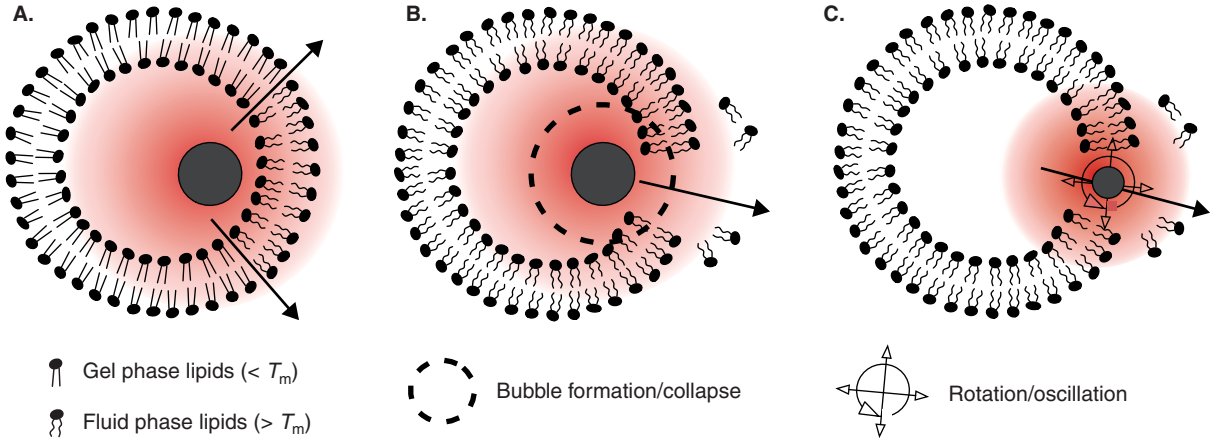

Figure 5. Controlled release mechanisms of LNAs. (A) Thermally-induced phase transitions due to NP heating where release is achieved through high diffusivity at the interface between gel and fluid lipid phases. **(B)** Mechanically-induced release where the bilayer is 'broken' due to bubble formation/rupture as a result of NP heating. **(C)** Mechanically-induced release where the bilayer is 'broken' due to NP rotation or oscillation at or within a LNA bilayer.
LNA: Liposome-nanoparticle assembly; NP: Nanoparticle.

and chemical properties of the liposome, the NP and the dispersing phase. Studies are needed that demonstrate the relationship among NP loading; liposome morphology, structure and stability; and bilayer permeability for different LNA designs.

- *Is the concept of local or nanoscale heating valid and under what conditions?* LNAs designed for controlled release usually report a local or nanoscale heating mechanism where the NPs transfer heat to the LNA and cause a phase change within the bilayer that triggers bilayer permeabilization. From this rationale, NPs in close proximity to bilayer, such as the case for embedment or decoration, would have the greatest effect on controlled release. However, other release mechanisms as a result of NP stimulation, working in tandem with bilayer heating, may be utilized (**Figure 5**). This statement is based in part on work by Keblinski *et al.* [65], who have shown that the theoretical temperature difference between an NP surface and the bulk phase due to EMF heating (light or RF) is almost negligible. This was further verified experimentally by Gupta *et al.* [97] and Bothun and Preiss [98] for Fe_3O_4 NPs heated by RF. The fact that little difference between nanoscale and bulk heating is observed is due to the negligible heat transfer resistance in nanoscale films and rapid heat dissipation from the NP surface. Hence, NP heating does indeed occur and can trigger LNA release, but the heating is not localized to the LNA and no measurable difference can be observed with the bulk phase. It is unlikely that a lipid bilayer, even in contact with the NP surface, would exhibit a different temperature than that of the surrounding aqueous phase.
- *What is LNA toxicity and how does the design strategy affect?* It is unclear if LNA toxicity will stem from the liposomes or the NPs, or if a synergistic effect will occur. Toxicity, which is important from a clinical perspective, will depend on the LNA design and associated colloidal stability. For example, toxicity could be 'low' if an LNA can retain its NP agent until it reaches a target site. This could be the case for bound NPs formed by embedment or encapsulation. However, 'higher' toxicity could occur if the NPs are released during circulation (i.e., toxicity of liposomes + NPs). Release of encapsulated NPs could be attributed to liposome fusion or bilayer disintegration, release of embedded NPs may occur due to bilayer solubilization by surface-active agents, and release of decorated NPs may occur due to charge screening or competitive binding.
- *What clinical challenges exist to LNA-based therapeutic assemblies?* As with toxicity, it is unclear if LNAs present unique clinical challenges beyond those reported for liposomes or NPs [3,4,22]. These challenges include achieving biocompatibility, bioavailability, and cellular targeting and uptake. LNA structure, function and stability will clearly impact how these challenges are addressed.

Declaration of interest

The authors declare no conflict of interest. This work was supported by grants from the National Science Foundation (CBET-0931875) and the NASA Rhode Island Space Grant Consortium.

Bibliography

Papers of special note have been highlighted as either of interest (•) or of considerable interest (••) to readers.

1. Koo OM, Rubinstein I, Onyuksel H. Role of nanotechnology in targeted drug delivery and imaging: a concise review. Nanomedicine 2005;1(3):193-212
2. Brayden DJ. Controlled release technologies for drug delivery. Drug Discov Today 2003;8(21):976-8
3. Petros RA, DeSimone JM. Strategies in the design of nanoparticles for therapeutic applications. Nat Rev Drug Discov 2010;9(8):615-27

• **A very nice recent review of nanoparticle design for therapeutic applications.**

4. Phillips MA, Gran ML, Peppas NA. Targeted nanodelivery of drugs and diagnostics. Nano Today 2010;5(2):143-59
5. National Cancer Institute. 2005. Available from: www.nano.cancer.gov.[Cited]
6. Babincova M, Cicmanec P, Altanerova V, et al. AC-magnetic field controlled drug release from magnetoliposomes: design of a method for site-specific chemotherapy. Bioelectrochemistry 2002;55(1-2):17-19

• **To our knowledge this is the first report on magnetoliposomes.**

7. De Cuyper M, Joniau M. Magnetoliposomes: formation and structural characterization. Eur Biophys J 1988;15:311-19
8. Kullberg M, Mann K, Owens JL. Improved drug delivery to cancer cells: a method using magnetoliposomes that target epidermal growth factor receptors. Med Hypotheses 2005;64(3):468-70
9. Shinkai M, Yanase M, Honda H, et al. Intracellular hyperthermia for cancer using magnetite cationic liposomes: in vitro study. Jpn J Cancer Res 1996;87:1179-83
10. Soenen SJH, Hodenius M, De Cuyper M. Magnetoliposomes: versatile innovative nanocolloids for use in biotechnology and biomedicine. Nanomed 2009;4(2):177-91

• **A thorough review of magnetoliposomes.**

11. Viroonchatapan E, Sato H, Ueno M, et al. Release of 5-fluorouracil from thermosensitive magnetoliposomes induced by an electromagnetic field. J Control Release 1997;46(3):263-71
12. Al-Jamal WT, Kostarelos K. Liposome-nanoparticle hybrids for multimodal diagnostic and therapeutic applications. Nanomed 2007;2(1):85-98

• **An excellent review of liposome-nanoparticle hybrids (or LNAs as referred to herein).**

13. Volodkin DV, Skirtach AG, Mohwald H. Near-IR remote release from assemblies of liposomes and nanoparticles. Angew Chem Int Ed 2009;48(10):1807-9
14. Drbohlavova J, Adam V, Kizek R, Hubalek J. Quantum dots – Characterization, preparation and usage in biological systems. Int J Mol Sci 2009;10(2):656-73
15. Fukumori Y, Ichikawa H. Nanoparticles for cancer therapy and diagnosis. Adv Powder Technol 2006;17(1):1-28
16. Laurent S, Forge D, Port M, et al. Magnetic iron oxide nanoparticles: synthesis, stabilization, vectorization, physicochemical characterizations, and biological applications. Chem Rev 2008;108(6):2064-110
17. Rotomskis R, Streckyte G, Karabanovas V. Nanoparticles in diagnostics and therapy: towards nanomedicine. Medicina (B Aires) 2006;42(7):542-58
18. Mornet S, Vasseur S, Grasset F, Duguet E. Magnetic nanoparticle design for medical diagnosis and therapy. J Mater Chem 2004;14:2161-75
19. Li JL, Gu M. Gold-nanoparticle-enhanced cancer photothermal therapy. IEEE J Sel Top Quant 2010;16(4):989-96
20. Pradhan P, Giri J, Rieken F, et al. Targeted temperature sensitive magnetic liposomes for thermo-chemotherapy. J Control Release 2010;142(1):108-21

• **Demonstrates potential synergistic effect of combined hyperthermia and drug release.**

21. Zhang SL, Li J, Lykotrafitis G, et al. Size-dependent endocytosis of nanoparticles. Adv Mater 2009;21(4):419-+
22. Immordino ML, Dosio F, Cattel L. Stealth liposomes: review of the basic science, rationale, and clinical applications, existing and potential. Int J Nanomed 2006;1(3):297-315
23. Chen YJ, Bose A, Bothun GD. Controlled release from bilayer-decorated magnetoliposomes via electromagnetic heating. ACS Nano 2010;4(6):3215-21
24. Paasonen L, Laaksonen T, Johans C, et al. Gold nanoparticles enable selective light-induced contents release from liposomes. J Control Release 2007;122(1):86-93

• **A comparitive study of photothermal release with different LNA designs.**

25. Yu Y, Anthony SM, Zhang L, et al. Cationic nanoparticles stabilize zwitterionic liposomes better than anionic ones. J Phys Chem C 2007;111:8233-6
26. Zhang LF, Granick S. How to stabilize phospholipid liposomes (using nanoparticles). Nano Lett 2006;6(4):694-8

• **Demonstrates how nanoparticle decoration can stabilize liposome dispersions.**

27. Babincova M, Sourivong P, Leszczynska D, Babinec P. Fullerenosomes: design of a novel nanomaterial for laser controlled topical drug release. Physica Medica 2003;19(3):213-16
28. Chen YJ, Bothun GD. Lipid-assisted formation and dispersion of aqueous and bilayer-embedded nano-C60. Langmuir 2009;25(9):4875-9
29. Doi Y, Ikeda A, Akiyama M, et al. Intracellular uptake and photodynamic activity of water-soluble [60]- and [70] fullerenes incorporated in liposomes. Chem Eur J 2008;14:8892-7
30. Hwang KC, Mauzerall D. Photoinduced electron-transport across a lipid bilayer mediated by C70. Nature 1993;361(6408):138-40
31. Ikeda A, Kikuchi J-I, inventors; National University Corporation Nara Institute of Science and Technology, Japan. assignee. Fullerene C70-containing liposome, method for producing the same, and use of the same. 2008

32. Ikeda A, Nagano M, Akiyama M, et al. Photodynamic activity of C70 caged within surface-cross-linked liposomes. Chem Asian J 2009;4:199-205

33. Ikeda A, Sato T, Kitamura K, et al. Efficient photocleavage of DNA utilising water-soluble lipid membrane-incorporated [60]fullerenes prepared using a [60] fullerene exchange method. Org Biomol Chem 2005;3(16):2907-9

34. Jeng U-S, Hsu C-H, Lin T-L, et al. Dispersion of fullerenes in phospholipid bilayers and the subsequent changes in the host bilayers. Physica B 2005;357:193-8

35. Niu SF, Manzerall D. Fast and efficient charge transport across a lipid bilayer is electronically mediated by C-70 fullerene aggregates. J Am Chem Soc 1996;118(24):5791-5

36. Babincova M, Sourivong P, Leszczynska D, Babinec P. Photodynamic therapy of pigmented melanoma B16 using sterically stabilized fullerenosomes. Laser Phys Lett 2004;1(9):476-8

37. Savarala S, Ahmed S, Ilies MA, Wunder SL. Formation and colloidal stability of DMPC supported lipid bilayers on SiO2 nanobeads. Langmuir 2010;26(14):12081-8

38. Troutier AL, Ladaviere C. An overview of lipid membrane supported by colloidal particles. Adv Colloid Interface 2007;133(1):1-21

39. Zhang LX, Sun XP, Song YH, et al. Didodecyldimethylammonium bromide lipid bilayer-protected gold nanoparticles: synthesis, characterization, and self-assembly. Langmuir 2006;22(6):2838-43

40. Kshirsagar NA, Pandya SK, Kirodian GB, Sanath S. Liposomal drug delivery system from laboratory to clinic. J Postgrad Med 2005;51(Suppl 1):S5-15

41. Samad A, Sultana Y, Aqil M. Liposomal drug delivery systems: an update review. Curr Drug Deliv 2007;4(4):297-305

42. Torchilin VP. Recent advances with liposomes as pharmaceutical carriers. Nat Rev Drug Discov 2005;4(2):145-60

43. Mulder WJM, Strijkers GJ, van Tilborg GAF, et al. Lipid-based nanoparticles for contrast-enhanced MRI and molecular imaging. Nmr Biomed 2006;19(1):142-64

44. Emerich DF, Thanos CG. The pinpoint promise of nanoparticle-based drug delivery and molecular diagnosis. Biomol Eng 2006;23:171-84

45. Groneberg DA, Giersig M, Welte T, Pison U. Nanoparticle-based diagnosis and therapy. Curr Drug Targets 2006;7(6):643-8

46. Jin S, Ye K. Nanoparticle-mediated drug delivery and gene therapy. Biotechnol Prog 2007;23:32-41

47. Michalet X, Pinaud FF, Bentolila LA, et al. Quantum dots for live cells, in vivo imaging, and diagnostics. Science 2005;307(5709):538-44

48. Babincova M, Altanerova V, Altaner C, et al. In vitro analysis of cisplatin functionalized magnetic nanoparticles in combined cancer chemotherapy and electromagnetic hyperthermia. IEEE T Nanobiosci 2008;7(1):15-19

49. Bangham AD, Standish MM, Watkins JC. Diffusion of univalent ions across the lamellae of swollen phospholipids. J Mol Biol 1965;13:238-52

50. Bangham AD, Horne RW. Negative staining of phospholipids and their structural modification by surface active agents as observed in the electron microscope. J Mol Biol 1964;8:660-8

51. Papahadjopoulos D, Ohki S. Stability of asymmetric phospholipid membranes. Science 1969;164(883):1075-7

52. Gregoriadis G. Drug entrapment in liposomes. FEBS Lett 1973;36(3):292-6

53. Pagano RE, Weinstein JN. Interactions of liposomes with mammalian-cells. Annu Rev Biophys Biomol Struct 1978;7:435-68

54. Huang X, El-Sayed IH, El-Sayed MA. Applications of gold nanorods for cancer imaging and photothermal therapy. Methods Mol Biol 2010;624:343-57

55. Oldenburg SJ, Jackson JB, Westcott SL, Halas NJ. Infrared extinction properties of gold nanoshells. Appl Phys Lett 1999;75(19):2897-9

56. Krpetic Z, Nativo P, See V, et al. Inflicting controlled nonthermal damage to subcellular structures by laser-activated gold nanoparticles. Nano Lett 2010;10(11):4549-54

57. Gannon CJ, Patra CR, Bhattacharya R, et al. Intracellular gold nanoparticles enhance non-invasive radiofrequency thermal destruction of human gastrointestinal cancer cells. J Nanobiotechnology 2008;6:2

58. Pankhurst QA, Connolly J, Jones SK, Dobson J. Applications of magnetic nanoparticles in biomedicine. J Phys D 2003;36:167-81

59. Brezovich IA. Low frequency hyperthermia. Med Phys Monograph 1988;16:82-111

60. Hildebrandt B, Wust P, Ahlers O, et al. The cellular and molecular basis of hyperthermia. Crit Rev Oncol Hematol 2002;43(1):33-56

61. Hsu MH, Su YC. Iron-oxide embedded solid lipid nanoparticles for magnetically controlled heating and drug delivery. Biomed Microdevices 2008;10(6):785-93

62. Ito A, Kuga Y, Honda H, et al. Magnetite nanoparticle-loaded anti-HER2 immunoliposomes for combination of antibody therapy with hyperthermia. Cancer Lett 2004;212(2):167-75

63. Pennes HH. Analysis of tissue and arterial temperature in the resting human forearm. J Appl Physiol 1948;1:93-122

64. Rast L, Harrison JG. Computational modeling of electromagnetically induced heating of magnetic manoparticle materials for hyperthermic cancer treatment. PIERS Online 2010;6(7):690-4

65. Keblinski P, Cahill DG, Bodapati A, et al. Limits of localized heating by electromagnetically excited nanoparticles. J Appl Phys 2006;100:5

• **One of the first studies challenging the concept of nanoscale heating by nanoparticles using electromagnetic fields.**

66. Xu RZ, Zhang Y, Ma M, et al. Measurement of specific absorption rate and thermal simulation for arterial embolization hyperthermia in the Maghemite-Gelled model. IEEE T Magn 2007;43(3):1078-85

67. Hong K, Friend DS, Glabe CG, Papahadjopoulos D. Liposomes containing colloidal gold are a useful probe of liposome-cell interactions.

Biochim Biophys Acta 1983;732(1):320-3

68. Zheng S, Zheng Y, Beissinger RL, Fresco R. Microencapsulation of hemoglobin in liposomes using a double emulsion, film dehydration rehydration approach. Biochim Biophys Acta Biomembr 1994;1196(2):123-30

69. Szoka F Jr, Papahadjopoulos D. Procedure for preparation of liposomes with large internal aqueous space and high capture by reverse-phase evaporation. Proc Natl Acad Sci USA 1978;75(9):4194-8

70. Wijaya A, Hamad-Schifferli K. High-density encapsulation of Fe3O4 nanoparticles in lipid vesicles. Langmuir 2007;23(19):9546-50

• **Demonstrates high-density encapsulation in magnetoliposomes.**

71. Lipowsky R, Dobereiner HG. Vesicles in contact with nanoparticles and colloids. Europhys Lett 1998;43(2):219-25

72. Pradhan P, Giri J, Banerjee R, et al. Preparation and characterization of manganese ferrite-based magnetic liposomes for hyperthermia treatment of cancer. J Magn Magn Mater 2007;311:208-15

73. Sabate R, Barnadas-Rodriguez R, Callejas-Fernandez J, et al. Preparation and characterization of extruded magnetoliposomes. Int J Pharm 2008;347(1-2):156-62

74. Gomes JFPS, Rank A, Kronenberger A, et al. Polyelectrolyte-coated unilamellar nanometer-sized magnetic liposomes. Langmuir 2009;25(12):6793-9

75. Jang H, Pell LE, Korgel BA, English DS. Photoluminescence quenching of silicon nanoparticles in phospholipid vesicle bilayers. J Photochem Photobiol A 2003;158:111-17

• **Describes the critical nanoparticle size for bilayer embedment (see also references [69,76-77]).**

76. Bothun GD. Hydrophobic silver nanoparticles trapped in lipid bilayers: size distribution, bilayer phase behavior, and optical properties. J Nanobiotechnology 2008;6:13

77. Al-Jamal WT, Al-Jamal KT, Tian B, et al. Lipid-quantum dot bilayer vesicles enhance tumor cell uptake and retention in vitro and in vivo. ACS Nano 2008;2(3):408-18

78. Bothun GD, Rabideau AE, Stoner MA. Hepatoma cell uptake of cationic multifluorescent quantum dot liposomes. J Phys Chem B 2009;113(22):7725-8

79. Park S-H, Oh S-G, Mun J-Y, Han S-S. Effects of silver nanoparticles on the fluidity of bilayer in phospholipid liposome. Colloid Surf B 2005;44:117-22

80. Park S-H, Oh S-G, Mun J-Y, Han S-S. Loading of gold nanoparticles inside the DPPC bilayers of liposome and their effects on membrane fluidities. Colloid Surf B 2006;48:112-18

81. Binder WH, Sachsenhofer R, Farnik D, Blaas D. Guiding the location of nanoparticles into vesicular structures: a morphological study. Phys Chem Chem Phys 2007;9(48):6435-41

82. Rasch MR, Rossinyol E, Hueso JL, et al. Hydrophobic gold nanoparticle self-assembly with phosphatidylcholine lipid: membrane-loaded and janus vesicles. Nano Lett 2010;10(9):3733-9

• **Depicts how embedded Au nanoparticles cluster in LNAs and how LNA preparation yields different structures.**

83. Ginzburg VV, Balijepalli S. Modeling the thermodynamics of the interaction of nanoparticles with cell membranes. Nano Lett 2007;7(12):3716-22

84. Wi HS, Lee K, Pak HK. Interfacial energy consideration in the organization of a quantum dot-lipid mixed system. J Phys Cond Mat 2008;20(49):1-6

85. Al-Jamal WT, Al-Jamal KT, Bomans PH, et al. Functionalized-quantum-dot-liposome hybrids as multimodal nanoparticles for cancer. Small 2008;4(9):1406-15

86. Wang B, Zhang LF, Bae SC, Granick S. Nanoparticle-induced surface reconstruction of phospholipid membranes. Proc Nat Acad Sci USA 2008;105(47):18171-5

• **A key study that demonstrates how nanoparticle binding to liposomes can induce phase separation.**

87. Sau TP, Urban AS, Dondapati SK, et al. Controlling loading and optical properties of gold nanoparticles on liposome membranes. Colloid Surf A 2009;342:92-6

• **Compares Au nanoparticle binding as a function of liposome surface charge.**

88. Kojima C, Hirano Y, Yuba E, et al. Preparation and characterization of complexes of liposomes with gold nanoparticles. Colloid Surf B 2008;66(2):246-52

89. Pornpattananangkul D, Olson S, Aryal S, et al. Stimuli-responsive liposome fusion mediated by gold nanoparticles. ACS Nano 2010;4(4):1935-42

90. Mart RJ, Liem KP, Webb SJ. Creating functional vesicle assemblies from vesicles and nanoparticles. Pharm Res 2009;26(7):1701-10

91. Anderson LJE, Hansen E, Lukianova-Hleb EY, et al. Optically guided controlled release from liposomes with tunable plasmonic nanobubbles. J Control Release 2010;144(2):151-8

92. Wu GH, Milkhailovsky A, Khant HA, et al. Remotely triggered liposome release by near-infrared light absorption via hollow gold nanoshells. J Am Chem Soc 2008;130(26):8175-7

• **Demonstrates ability to use encapsulated or decorated hollow Au nanoshells for laser-triggered release.**

93. Tai LA, Tsai PJ, Wang YC, et al. Thermosensitive liposomes entrapping iron oxide nanoparticles for controllable drug release. Nanotechnology 2009;20:13

94. Chithrani DB, Dunne M, Stewart J, et al. Cellular uptake and transport of gold nanoparticles incorporated in a liposomal carrier'. Nanomed Nanotechnol 2010;6(1):161-9

95. Paasonen L, Sipila T, Subrizi A, et al. Gold-embedded photosensitive liposomes for drug delivery: triggering mechanism and intracellular release. J Control Release 2010;147(1):136-43

96. Babinec P, Babincova M, Sourivong P, Leszczynska D. Efficient treatment of pigmented B16 melanoma using photosensitized long-circulating magnetofullerenosomes. J Magn Magn Mater 2005;293(1):394-7

97. Gupta A, Kane RS, Borca-Tasciuc DA. Local temperature measurement in the vicinity of electromagnetically heated magnetite and gold nanoparticles. J Appl Phys 2010;108:6

98. Bothun GD, Preiss MR. Bilayer heating in magnetite nanoparticle–liposome dispersions via fluorescence anisotropy. J Colloid Interface Sci 2011;In press

99. Larsen BA, Haag MA, Serkova NJ, et al. Controlled aggregation of

superparamagnetic iron oxide nanoparticles for the development of molecular magnetic resonance imaging probes. Nanotechnology 2008;19:26

100. Zhu L, Huo ZL, Wang LL, et al. Targeted delivery of methotrexate to skeletal muscular tissue by thermosensitive magnetoliposomes. Int J Pharm 2009;370(1-2):136-43

Affiliation

Matthew R Preiss & Geoffrey D Bothun†
†Author for correspondence
University of Rhode Island,
Department of Chemical Engineering,
Rhode Island Consortium for Nanoscience and Nanotechnology,
16 Greenhouse Road,
Kingston, RI 02881, USA
Tel: +1 401 874 9518;
E-mail: bothun@egr.uri.edu